Supporting Information

Synthesis and Characterization of Ultralong Copper Sulfide Nanowires and their Electrical Properties

Cosimo Anichini,[a] Włodzimierz Czepa[b,c] Alessandro Aliprandi,[a] Valentina Girelli Consolaro,[d] Ovidiu Ersen,[d]

Artur Ciesielski[a,b,] Paolo Samorì[a*]*

[a] *Université de Strasbourg, CNRS, ISIS 8 allée Gaspard Monge, 67000 Strasbourg, France.*

E-mail : ciesielski@unistra.fr, samori@unistra.fr

[b] *Centre for Advanced Technologies, Adam Mickiewicz University, 61-614 Poznań, Uniwersytetu Poznańskiego 10, Poland.*

[c] *Faculty of Chemistry, Adam Mickiewicz University, Uniwersytetu Poznańskiego 8, 61-614 Poznań, Poland.*

[d] *Université de Strasbourg,CNRS, IPCMS, 23 rue du Loess, BP 43 67034 Strasbourg Cedex 2, France*

Table of Contents

Instrumental methods

For X-Ray Photoelectron Spectroscopy (XPS) measurements Cu2-xSNWs were deposited by drop-casting onto silicon substrates. The X-Ray Photoelectron Spectroscopy (XPS) measurements were carried out using a Thermo Scientific KAlpha X-ray Photoelectron Spectrometer system equipped with an Al Kα X-Ray source (photon energy Eph = 1486.6 eV, beam spot size ~100 µm). The depth profiling was done by etching the Cu2-xSNWs with a rastered Argon ions beam (2 kV). Transmittance UV-Vis spectra of the substrates were recorded on the Jasco V-670 spectrophotometer. Raman spectra were recorded by a Renishaw microscope with a 50x objective, laser excitation wavelength of 532 nm and laser power of 1% on Cu2-xS NWs deposited on Si substrate. The silicon peak at 520.3 cm^{-1} was taken as reference for wavenumber calibration. TGA was conducted using a Mettler Toledo TGA/DSC 2 system, with a heating rate of 10 °C min^{-1} from 25 °C to 800 °C under air atmosphere. The X-Ray Diffraction (XRD) measurements were performed in specular geometry using a SmartLab-Rigaku diffractometer equipped with a rotating anode (Cu Kα, λ = 1.54180 Å), followed by a parabolic mirror to collimate the incident beam, and a series of variable slits (placed before and after the sample position). Scanning Electron Microscopy (SEM) was performed with a FEI Quanta 250 FEG instrument, operated in high vacuum mode (pressure in 10^{-4} Pa range). Conventional transmission electron microscopy (TEM), high resolution TEM (HRTEM) imaging, electron diffraction (ED) and Energy-Dispersive X-Rays Spectroscopy (EDX) were performed a JEOL2100F microscope operating at 200 kV and equipped with a probe corrector for spherical aberrations. Photoemission spectroscopy in air (PESA) measurements were performed on Cu2-xSNWs drop-casted on a Si/SiO_2 substrate (230 nm) with an AC-2 Photoelectron Spectrometer (Riken-Keiki Co.). A UV light intensity of 40 nW and a counting time of 10 seconds per point were used for the measurement. All the electrical measurements were performed with a Keithley 2636A source meter, except the measurements of sheet resistance, which were performed with a Jandel RM3000 test unit equipped with a four-point probe.

Results and Discussion

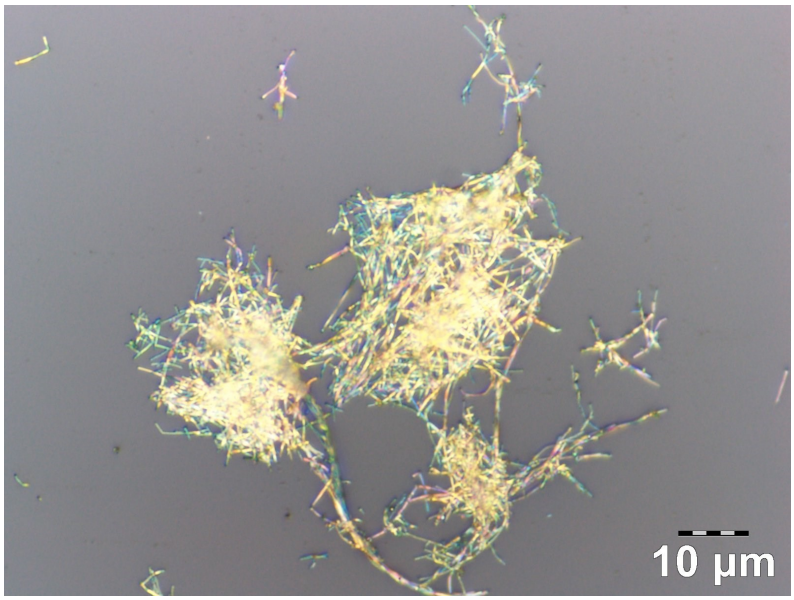

Figure S1. Optical micrograph of Cu NWs treated with a 30mM water solution of thiourea at 90 °C for 30 min.

Energy-dispersive X-ray spectroscopy (EDX)

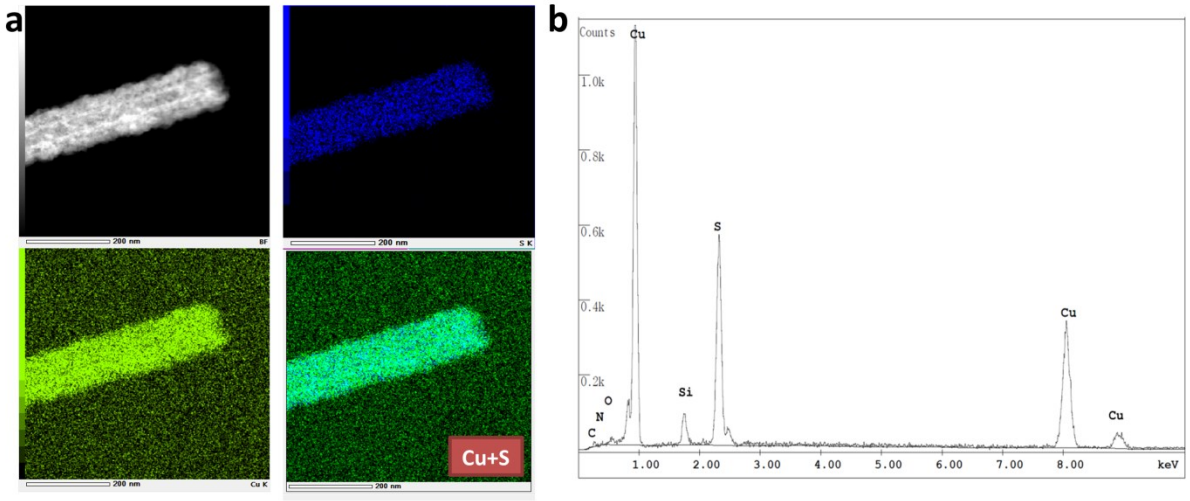

Figure S2. (a) EDX mapping of a $Cu_{2-x}S$ NW (gray, the high angle annular dark field image, blue: S chemical map, green: Cu chemical map). (b) Representative EDX spectrum of $Cu_{2-x}S$ NWs.

X-ray photoelectron spectroscopy (XPS)

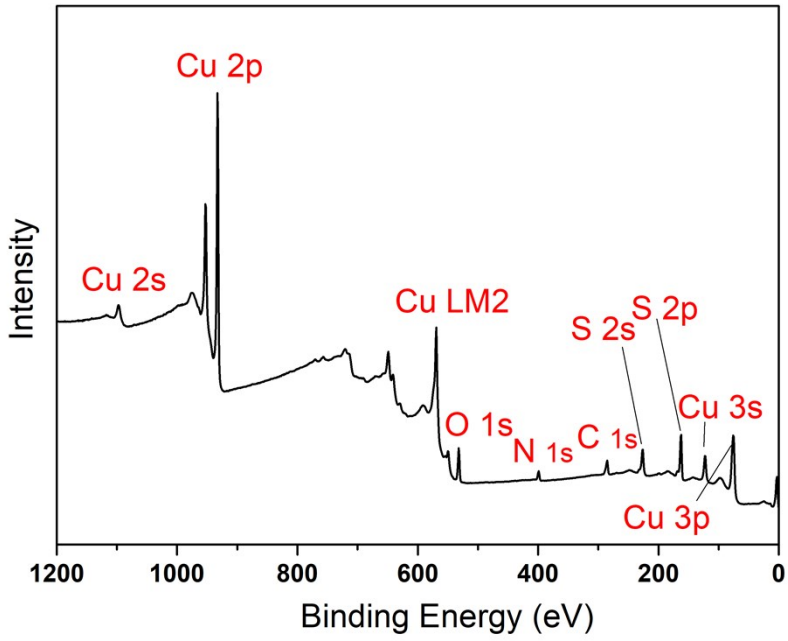

Figure S3. XPS survey spectrum of $Cu_{2-x}S$NWs.

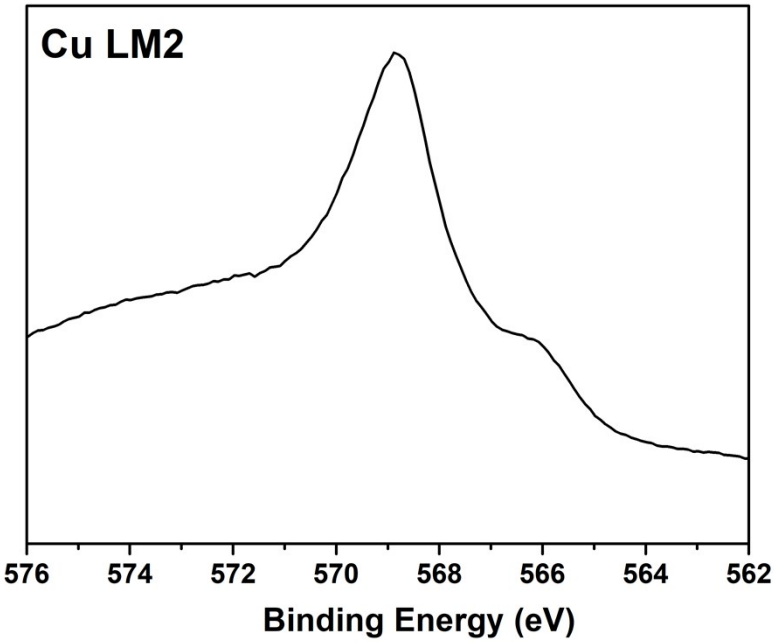

Figure S4. XPS spectrum of Cu LM2 peak of Cu_{2-x}SNWs.

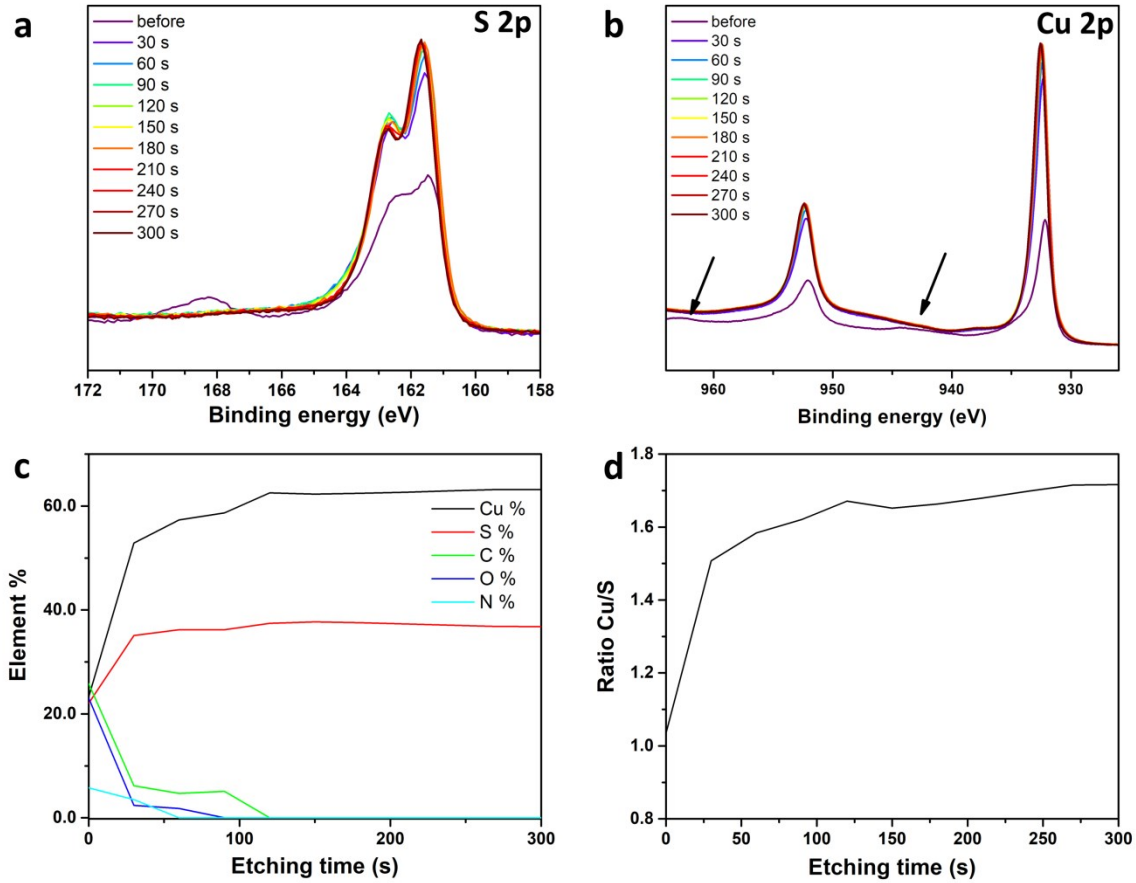

Figure S5. S 2p spectra (a) and Cu 2p spectra (b) of Cu_{2-x}SNWs before and after increasing times of exposure (30-300 s) to an accelerated Argon ions beam. Element abundance (%) computed from the Survey spectra (c) and elemental ratio Cu/S (d) as a function of the Ar^+ etching time.

UV-Vis Absorbance

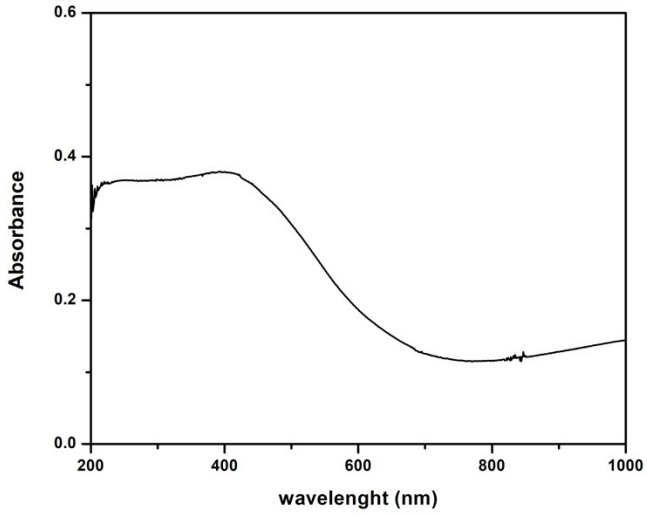

Figure S6. Absorbance spectrum of Cu_{2-x}SNWs dispersed in ethanol.

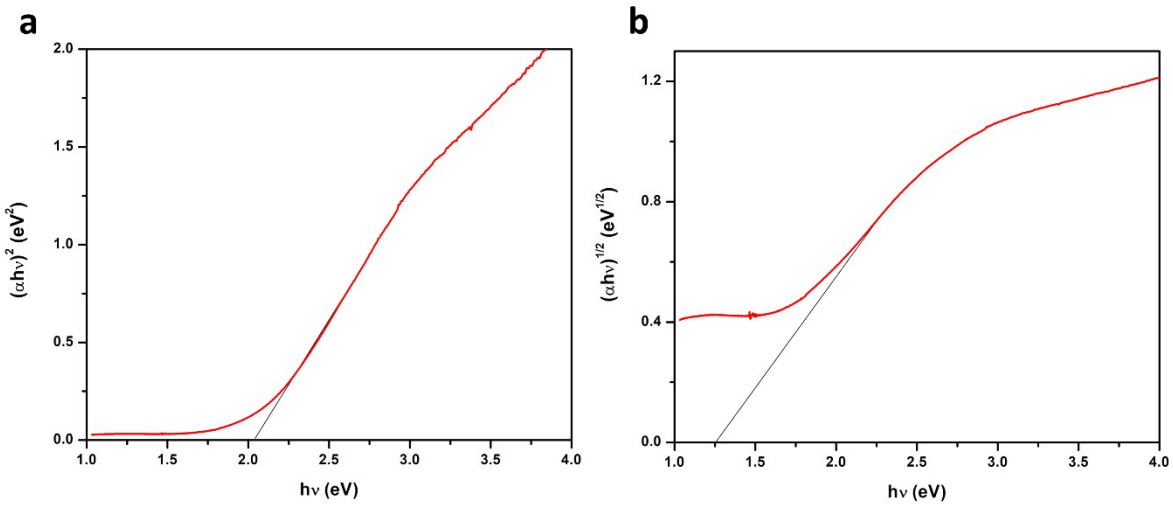

Figure S7. Tauc plots for direct (a) and indirect (b) band-gaps of $Cu_{2-x}S$NWs dispersed in ethanol.

Photoelectron spectroscopy in air (PESA)

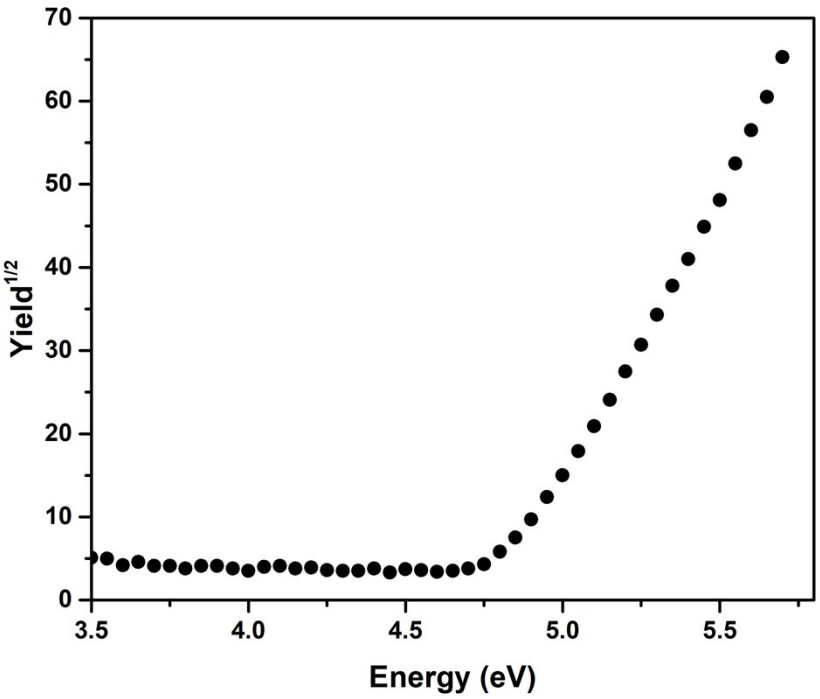

Figure S8. Measurements of the ionization energy of $Cu_{2-x}S$ NWs by photoemission spectroscopy in air (PESA)

Bending tests

First, $Cu_{2-x}S$ NWs were spray coated onto PEN substrates (1.5x5.0 cm^2, 125 µm thick) and the film was contacted electrically with conductive copper tape and Ag paste. The sheet resistance of the films was 2.4 kΩ/sq. The stability of the film to the bending was first characterized by performing sheet resistance measurements under different bending radii, using 3D printing molds with different well-defined diameters. The electrical resistivity was measured in situ with the film kept at the desired bending radius. The stability of the $Cu_{2-x}S$ NWs conductive film to fatigue bending has been carried out by performing 10000 bending cycles using a digital force gauge (Mark-10, M7-025E, ~25 N) equipped with a motorized test stand (Mark-10, ESM-

303E). In each bending cycle the gauge was extended of 5 mm (Figure S10). The corresponding bending radius was measured with a caliper and was equal to 8 mm. All the above-mentioned tests were performed by applying a bias voltage of 0.1 V.

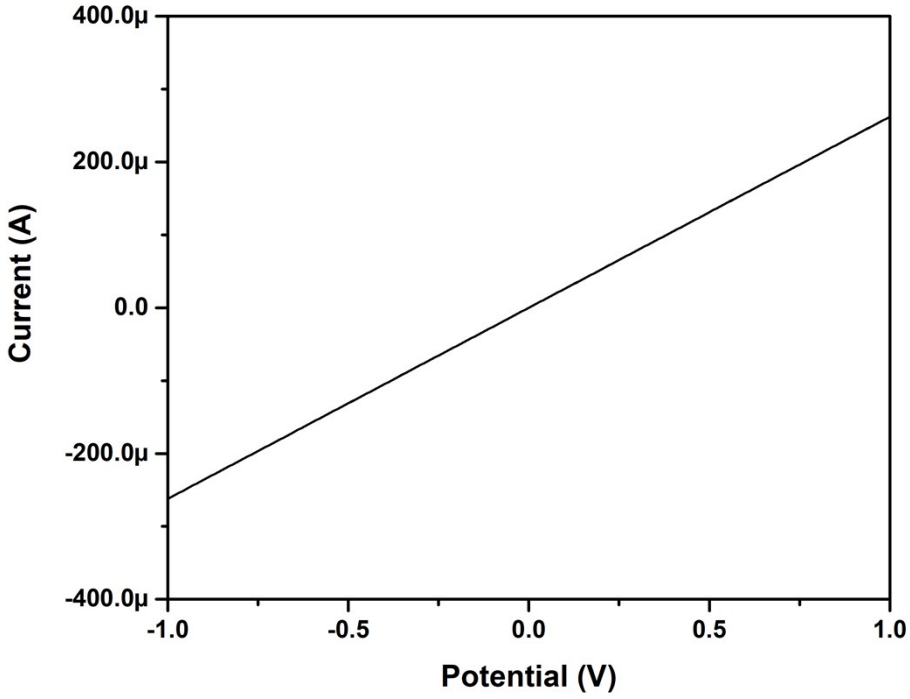

Figure S9. I-V characteristic of a Cu_{2-x}SNWs spray-coated film on PEN

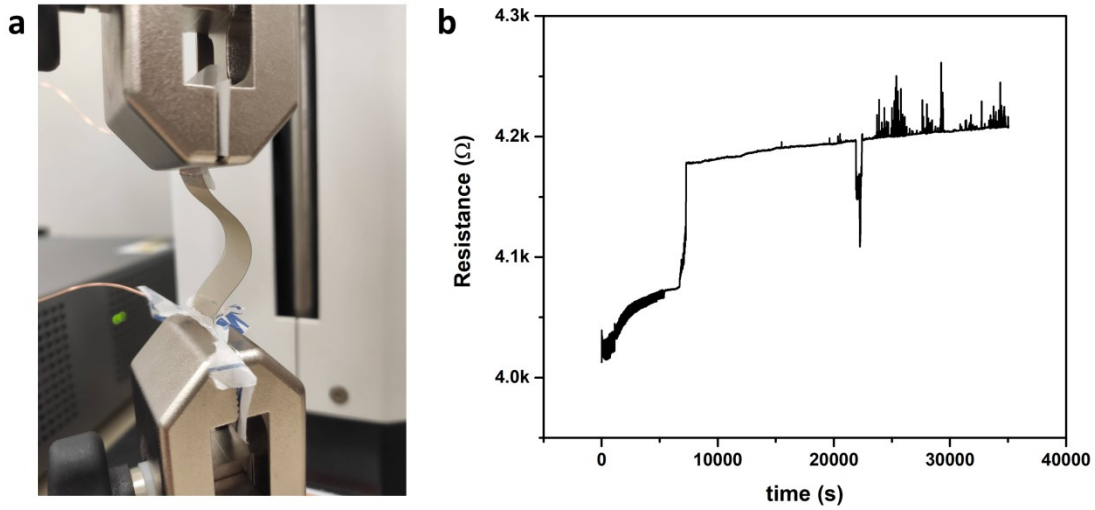

Figure S10. a) Photo of the 5x1.5 cm^2 conductive film of spray-coated Cu_{2-x}SNWs on PEN (125µm) in the bent position (8 mm radius). (b) Resistance of the film as a function of time during the application of 10000 bending cycles with a bending radius of 8 mm.

Sheet resistance as a function of transmittance

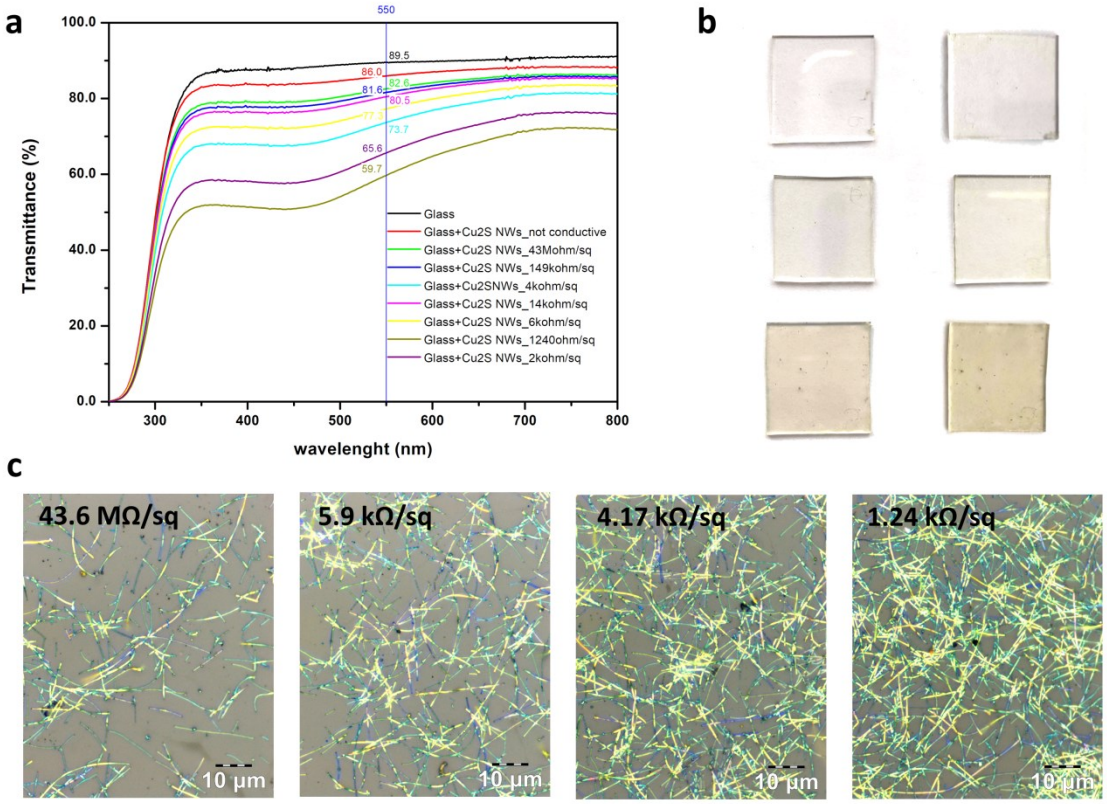

Figure S11. Transmittance spectra (a), photos (b) and microphotographs (c) of the glass substrate with increasing amounts of spray-coated $Cu_{2-x}S$ NWs.

Corrosion resistance

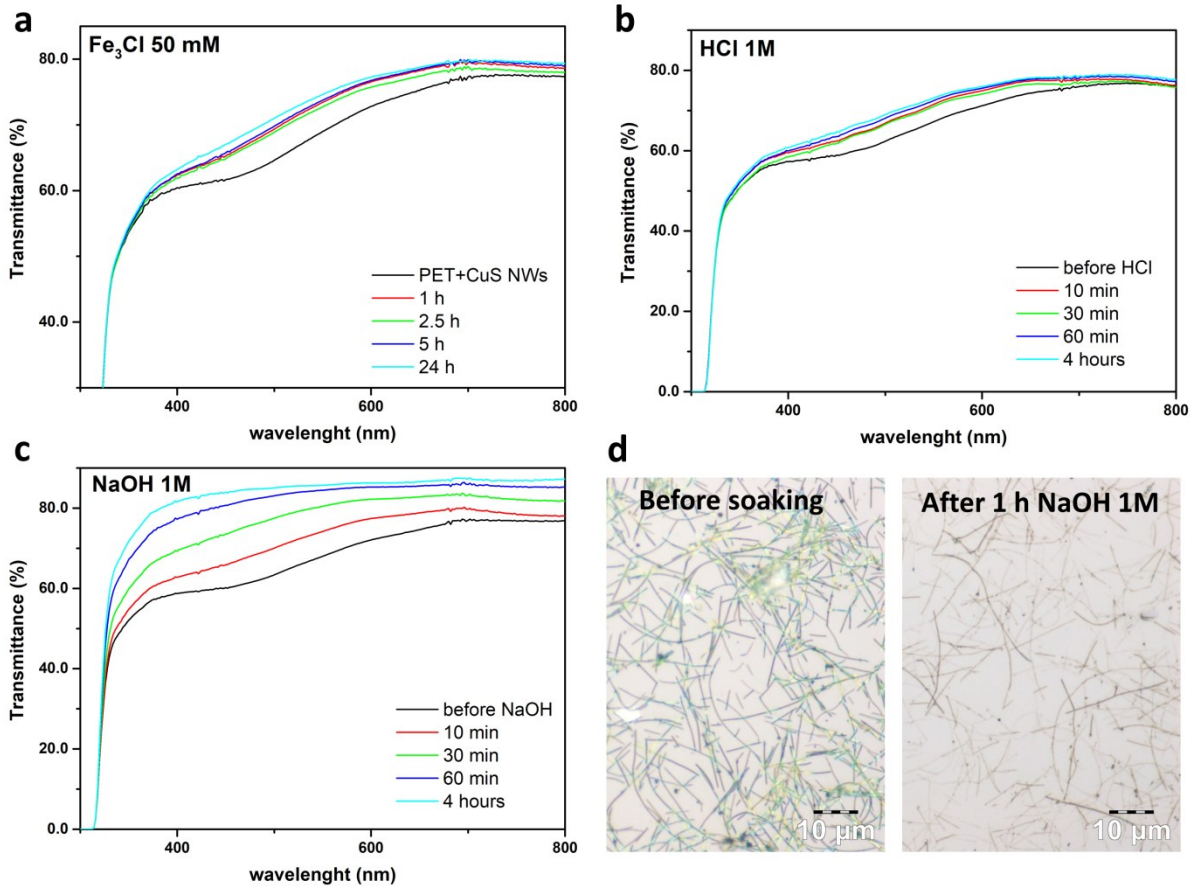

Figure S12. Transmittance spectra of spray-coated Cu_{2-x}SNWs on glass before and after increasing exposure times to water solutions of $FeCl_3$ 50 mM (a), HCl 1M (b), NaOH (c). (d) Micrograph of spray-coated Cu_{2-x}SNWs on glass before and after 1h of exposure to a 1 M water solution of NaOH.

DSC and TGA

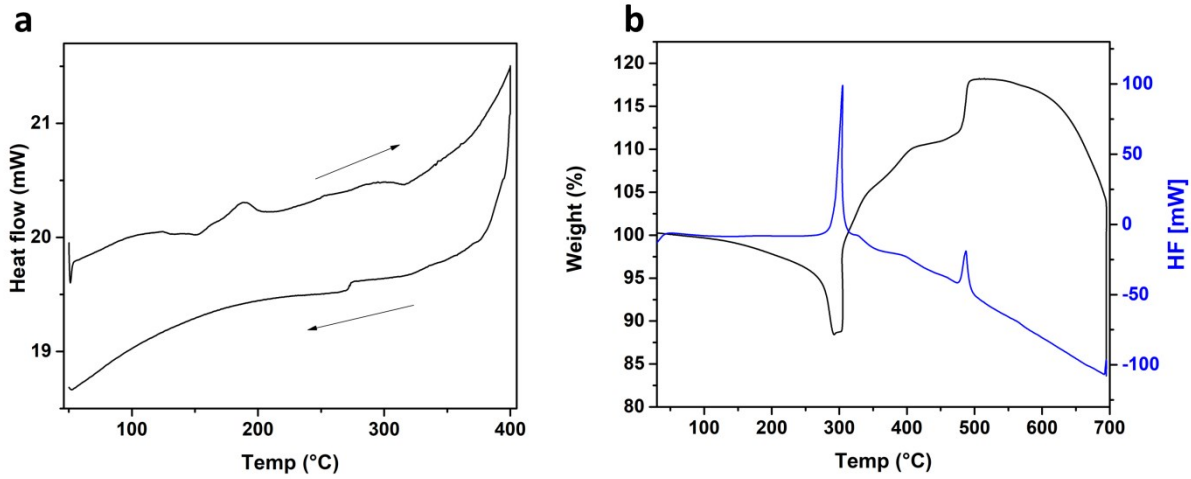

Figure S13. (a) DSC performed under Nitrogen flux (heating and cooling, 5 °C/min) ands (b) TGA-DSC performed under air (heating, 10 °C/min) of Cu_{2-x}SNWs.

XPS before and after annealing under N2 at 190°C for 30 min

In Figure S14a-b are reported the Cu 2p peak and S 2p peak of Cu_{2-x}SNWs before and after the annealing at 190 °C. It is possible to notice that after the annealing the two weak satellites peaks at 944 and 963 eV due to the presence of Cu^{2+} disappear completely, indicating a removal of the surface oxidized layer after the annealing. Similarly, also the peak at 168.3 eV in the S 2p region, due to the presence of sulfate, disappears completely after the annealing. Furthermore, the elemental abundance calculated from the fitting of XPS survey spectra of the Cu_{2-x}SNWs before and after the annealing (Figure S 14c) shows an important reduction of C and O after the annealing, which indicates a desorption of the organic contaminants (thiourea byproducts and solvent) and a reduction of the surface oxidized layer.

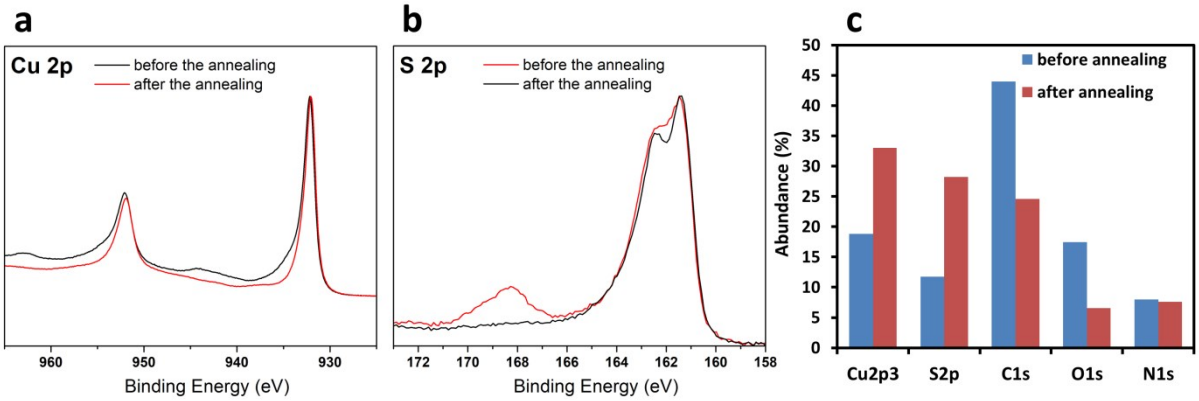

Figure S14. XPS spectra of Cu 2p (a) and S 2p (b) regions of Cu_{2-x}SNWs before (red) and after (black) annealing under nitrogen (190 °C, 30 min). (c) Abundance of the elements Cu, S, C, O and N, computed from the fitting of XPS survey spectra, in the Cu_{2-x}SNWs sample before and after the annealing.

Single nanowire device

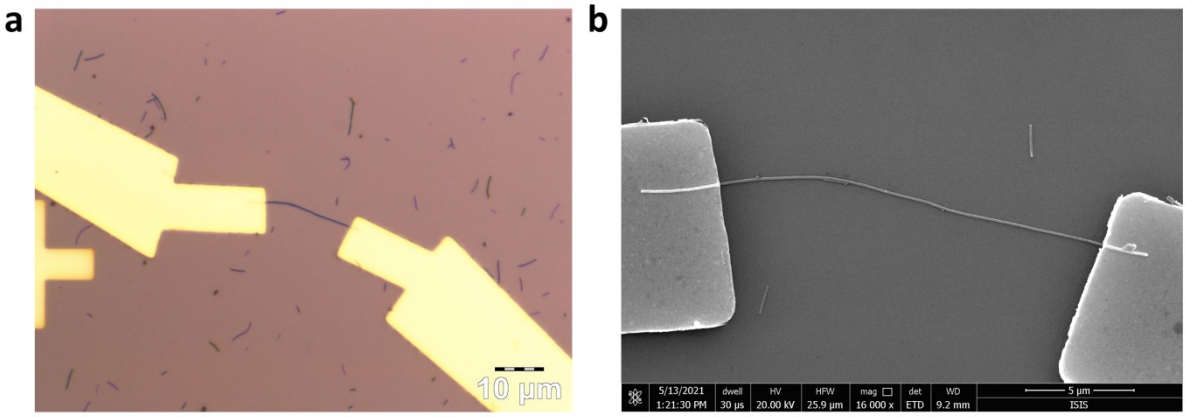

Figure S15. Optical micrograph (a) and SEM image (b) of the single Cu_{2-x}S NW device, showing the two gold electrodes.

Electrochemical characterization of the Cu_{2-x}S NWs based supercapacitor

Cyclic voltammetry (CV) was performed in the range of 0-2.5 V in the range of scan rates ranging from 5 mV s^{-1} to 2000 mV s^{-1}. The specific and volumetric capacitance were calculated from the CV curves using following equation[1]:

$$C = \frac{\int ivdv}{2\mu k \Delta V}$$

where, i and v are current and potential in the CV tests, μ is the scan rate of measurement (V/s), k is either the mass of active material (for specific capacitance) or its volume (for volumetric capacitance) and ΔV is the potential window. The volume of the electrode was calculated from its area and average thickness, which were, respectively, 350 μm and 1.53 cm^2. The average thickness of the electrode was measured with a KLA-Tencor Alpha-Step IQ profilometer.

The energy density was calculated according to the following equation:

$$E = \frac{1}{2} \times C \times \frac{\Delta V}{3600}$$

where E is the energy density (Wh cm^{-3}), C is the volumetric capacitance, ΔV is the discharge voltage range.

Galvanostatic charge-discharge curves (GCD) were recorded from 0-2.5 V at different current densities (1-10 A g^{-1}). Electrochemical Impedance Spectroscopy was taken in the frequency range from 100 kHz to 1 mHz with an amplitude of 10 mV. CV, GCD curves and EIS were recorded using EC-LAB VMP3 (BioLogic Science Instrument).

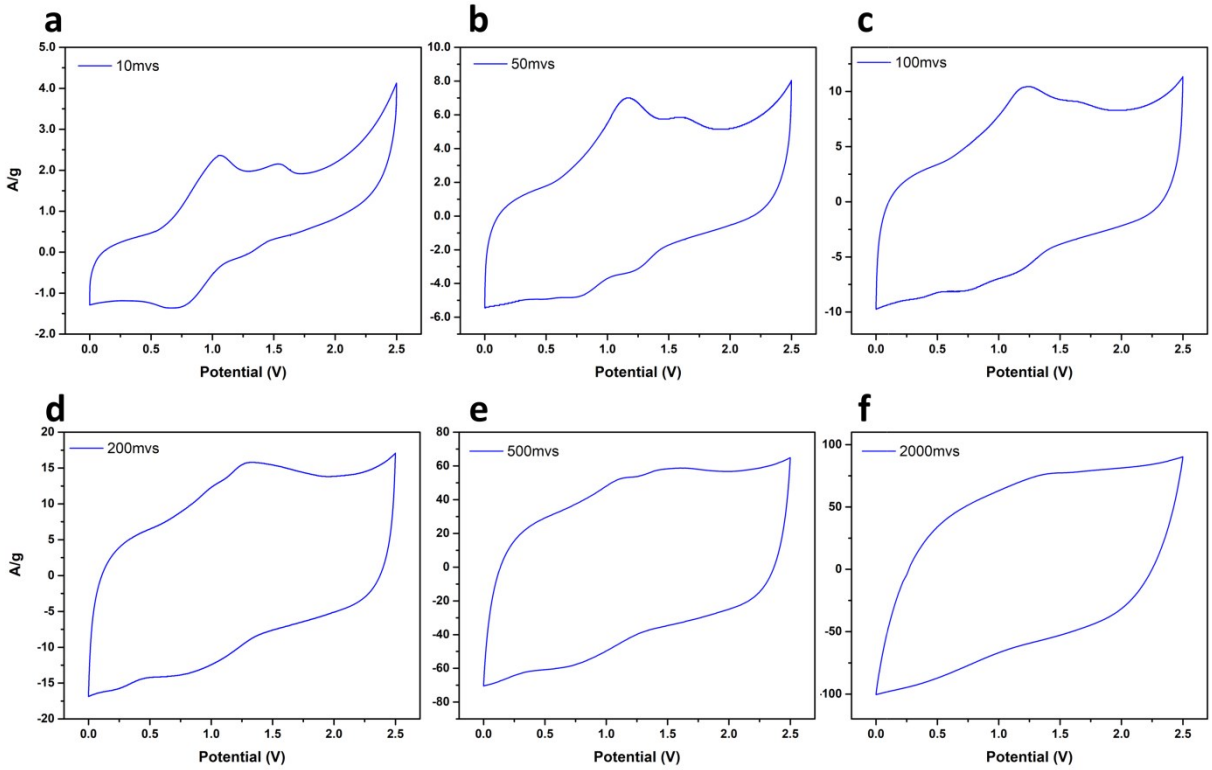

Figure S16. Cyclic voltammetry (CV) curves of the $Cu_{2-x}S$ NWs based supercapacitor at different scan rates: 10 mV/s (a), 50 mV/s (b), 100 mV/s (c), 200 mV/s (d), 500 mV/s (e) and 2000 mV/s (f).

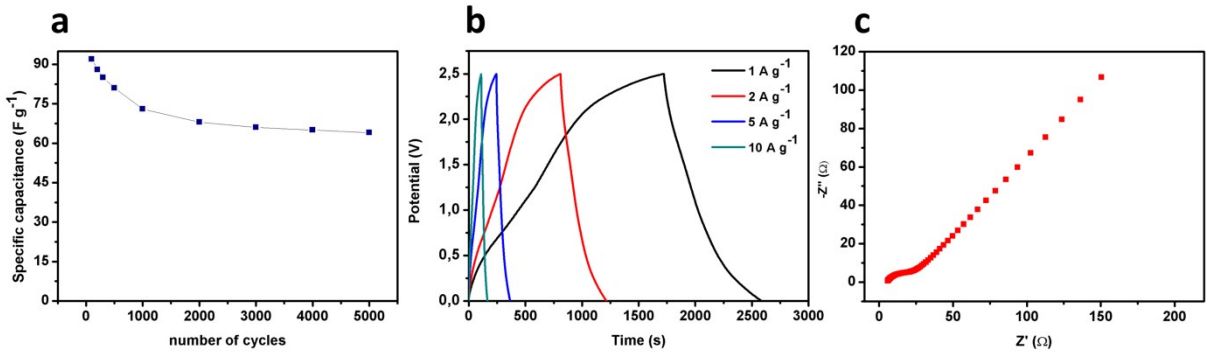

Figure S17. (a) Specific capacitance of the $Cu_{2-x}S$ NWs based supercapacitor as a function of the number of CV cycles (scan rate 100 mV/s). (b) Galvanostatic charge-discharge (GCD) curves of the supercapacitor at 1, 2, 5 and 10 A/g. (c) Electrochemical impedance spectroscopy (EIS) Nyquist plot of the supercapacitor.

Table S1. Specific and volumetric capacitance of the electrode at different scan rates

Scan Rate [mV s^{-1}]	Specific Capacitance [F g^{-1}]	Volumetric Capacitance [F cm^{-3}]
5	324	60,5
10	270	50,4
50	144	26,9
100	91	17,0
200	70	13,1
500	42	7,8
1000	40	7,5

References

1. Zhang, L.; Gong, H. Improvement in flexibility and volumetric performance for supercapacitor application and the effect of Ni–Fe ratio on electrode behaviour. *Journal of Materials Chemistry A* **2015,** *3* (14), 7607-7615.